One-Dimensional Anomalous Diffusion of Gold Nanoparticles in a Polymer Melt

Jing-Jin Song, Rupak Bhattacharya, Hyunki Kim, Jooyoung Chang, Tsung-Yeh Tang, Hongyu Guo, Sajal K. Ghosh, Yi Yang, Zhang Jiang, Hyeyoung Kim, Thomas P. Russell, Gaurav Arya, Suresh Narayanan, and Sunil K. Sinha

Phys. Rev. Lett. **122**, 107802 — Published 15 March 2019

DOI: 10.1103/PhysRevLett.122.107802

One-Dimensional Anomalous Diffusion of Gold Nanoparticles in a Polymer Melt*

Jing-Jin Song‡
Department of Materials Science & Engineering, University of California San Diego, 9500 Gilman Dr. La Jolla, CA, 92093, USA.

Rupak Bhattacharya‡, Yi Yang, Sajal K. Ghosh, and Sunil K. Sinha*†
Department of Physics, University of California San Diego, 9500 Gilman Dr. La Jolla, CA, 92093, USA.

Hyunki Kim, Jooyoung Chang, Hyeyoung Kim, and Thomas P. Russell
Polymer Science and Engineering Department,University of Massachusetts Amherst, Amherst MA, 01003, USA.

Tsungyeh Tang and Gaurav Arya
Department of NanoEngineering, University of California San Diego, 9500 Gilman Dr. La Jolla, CA, 92093, USA.

Hongyu Guo
National Institute of Standards and Technology, 100 Bureau Dr., Stop 1070, Gaithersburg, MD, 20899, USA.

Suresh Narayanan and Zhang Jiang
Advanced Photon Source, Argonne National Laboratory, 9700 Cass Ave, Lemont, IL 60439, USA.

(Dated: February 5, 2019)

We investigated the dynamics of polymer-grafted gold nanoparticles loaded into polymer melts using X-ray photon correlation spectroscopy. For low molecular weight host matrix polymer chains, normal isotropic diffusion of the gold nanoparticles is observed. For larger molecular weights, anomalous diffusion of the nanoparticles is observed that can be described by ballistic motion and generalized Levy walks, similar to those often used to discuss the dynamics of jammed systems. Under certain annealing conditions, the diffusion is one-dimensional and related to the direction of heat flow during annealing and is associated with an dynamic alignment of the host polymer chains. Molecular dynamics simulations of a single gold nanoparticle diffusing in a partially aligned polymer network semi-quantitatively reproduce the experimental results to a remarkable degree. The results help to showcase how nanoparticles can under certain circumstances move rapidly in polymer networks.

PACS numbers:

Functionalized metal nanoparticles (NPs) dispersed in a polymer matrix have been of considerable interest recently. Dilute dispersions of NPs in polymers can serve as a unique microrheological probe of the dynamics of the host polymer matrix, while at higher concentrations polymer nanocomposites (PNCs) are formed, which can exhibit a variety of complex thermal, mechanical, rheological, plasmonic, optical and electrical properties [1–9]. Ensuring effective dispersion of the NPs is one of the key issues in synthesizing PNCs [10]. Consequently, the motion of the functionalized NPs in the embedding matrix is also of intrinsic interest because it reveals how the NPs disperse at a microscopic level inside the polymer when it is in the melt state.

It is known that functionalized nanoparticles introduced into a polymer matrix show several different regimes of diffusion, ranging from classic Brownian motion to highly anomalous diffusion depending on the degree of entanglement of the chains anchored to the NP's with the host polymer chain [11–26]. Of particular interest is the regime where the nanoparticle size is comparable to the mesh size, which is the case explored here. Dynamical measurements may be made using multi-speckle dynamic light scattering (DLS) [11], photoluminescence or fluorescence correlation spectroscopy [12, 13] or its X-ray analog, known as X-ray photon correlation spectroscopy (XPCS) [14–24]. For NPs in polymer solutions, subdiffusive behavior has been observed [12, 17]. For polystyrene (PS) melts, Guo et al. [20] found normal hydrodynamic diffusion of Au NPs at high tem-

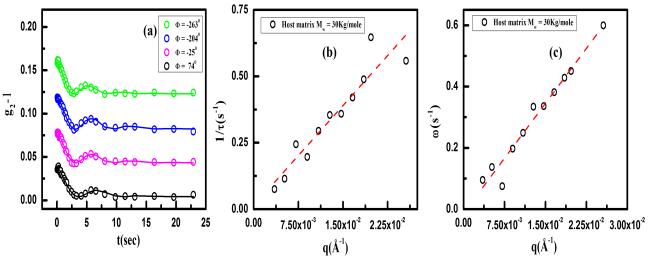

FIG. 1. (a) Isotropic (g_2 - 1) functions for 18 nm gold particle in host Matrix MW=30 Kg/mole for T = 160C and q = 9× 10^{-3}Å^{-1}. The curves have been vertically displaced for clarity. (b) $1/\tau$ vs q and (c) ω vs q for the above mentioned system.

peratures for host matrices of low to intermediate MW, while a crossover to hyperdiffusion with ballistic-like motion occurred as the temperature was lowered to below ∼1.1 T_g. Similar behavior was seen for alumina NPs in Polymethyl-methacrylate (PMMA) host matrices [19]. This behavior may be attributed to the onset of glassy behavior in the host matrix. Narayanan et al. studied the dynamics of Au NPs at the surface of thin films of PS at temperatures well above T_g and observed almost normal diffusion when the host matrix had a MW of 30 Kg/mole but ballistic-like motion for higher MW host PS chains [22].

In DLS or XPCS experiments, one measures the normalized scattered intensity autocorrelation function

$$g_2(\mathbf{q},t) = \frac{\langle I(\mathbf{q},t')I(\mathbf{q},t'+t)\rangle}{\langle I(\mathbf{q},t')\rangle^2} = 1 + A\,|f(\mathbf{q},t)|^2 \quad (1)$$

where $I(\boldsymbol{q},t)$ is the scattered intensity at time t, $\boldsymbol{q}$ is the wave vector transfer, the averages are over time t', and A $(0 < A < 1)$ is the instrumental coherence factor (with $A = 1$ for complete coherence of the beam). $f(\boldsymbol{q},t)$ is the normalized intermediate scattering function (ISF) related to the Fourier transform of the scattering function $S(\boldsymbol{q}, \omega)$ and for uncorrelated particles is given by

$$f(\mathbf{q},t) = \frac{1}{N}\sum_i \left\langle e^{-i\mathbf{q}.\mathbf{r}_i(0)} e^{i\mathbf{q}.\mathbf{r}_i(t)} \right\rangle \quad (2)$$

where $\boldsymbol{r}_i(t)$ is the position of particle i at time t and the bracket denotes an ensemble average. For studies of the motion of NPs in polymers, the ISF generally has been fit with the form (isotropic in $\boldsymbol{q}$)

$$f(\mathbf{q},t) = Ce^{-(t/\tau(q))^\beta} \quad (3)$$

where for normal diffusion, the exponent β =1 where D is the diffusion constant and $\tau(\boldsymbol{q}) = [Dq^2]^{-1}$. The hyperdiffusive behavior observed previously for Au NPs in PS melts in certain regimes is usually associated with $\beta > 1$ and $\tau(\boldsymbol{q}) = [Vq]^{-1}$, where V has the dimensions of a velocity related to a drift velocity of the NP, acquired due to the release of stresses at random locations in the host matrix, as is believed to occur in jammed systems. An oscillatory g_2 function can arise from uniform convective motion of the nanoparticles, if the scattered beam were heterodyning with some static reference beam [27–29], or in homodyning from shear flow [30], or a symmetric particle velocity distribution with a predominant magnitude of drift velocity. From Eq. (2),

$$\begin{aligned} f(\mathbf{q},t) &= \frac{1}{N}\sum_i \left\langle e^{i\mathbf{q}.[\mathbf{r}_i(t)-\mathbf{r}_i(0)]} \right\rangle = \frac{1}{N}\sum_i \left\langle e^{i\mathbf{q}.\mathbf{v}_i t} \right\rangle \\ &= \frac{1}{N}\sum_i \left\langle e^{i\mathbf{s}.\mathbf{v}_i} \right\rangle = \int d\mathbf{v} P(\mathbf{v}) e^{i\mathbf{v}.\mathbf{s}} \end{aligned} \quad (4)$$

where we have defined the vector variable $\boldsymbol{q}t$ by $\boldsymbol{s}$ and $P(\boldsymbol{v})$ is the velocity distribution for the particles. If $P(\boldsymbol{v})$ is peaked around one particular magnitude of the velocity v, this will give rise to an oscillatory $f(\boldsymbol{q},t)$[31]. From Eq.(4), $P(\boldsymbol{v})$ can be obtained from the Fourier transform of $f(\boldsymbol{q},t)$ with respect to $\boldsymbol{s}$. In this case, Fourier transforming $f(\boldsymbol{q},t)$ can yield the distribution of particle drift velocities [27, 32], as illustrated below. In several previous studies, β was found to be dependent on both q and temperature, and in some cases $\tau(q)$ was found to crossover between the forms given above at some values of q [14, 22]. Possible anisotropies in the particle motion or oscillatory g_2 functions have never been explored previously in the case of NPs in polymers.

In the present work, we report the results of XPCS studies of functionalized Au NPs dispersed in molten PS that illustrates several such novel features, including anisotropy effects, drift velocities, and the effect of stress in the host polymer network. We also present the results of molecular dynamics simulations, which agree well with our experimental results and demonstrate the intermittent random ballistic-like motion seen here.

The volume fraction of the NPs was very small, so as to minimally perturb the host polymer. Two different sizes of Au NPs (13 nm and 18 nm diameter), were densely grafted with ligands of linear PS of MW 38 Kg/mole to prevent aggregation, and dispersed at a volume concentration of 0.5% in host matrices of linear PS of MWs of 13 Kg/mole (T_g∼ 90C), 30 Kg/mole and 97 Kg/mole (T_g∼ 100C) respectively, were studied as a function of temperature. The high grafting density of the ligand chains (see SI) implies that they form a brush and thus only the 13 Kg/mole host matrix chains can penetrate and wet the NPs [33, 34].

Details of the synthesis and functionalization of the gold nanoparticles are described in the Supplementary Information (SI) section [35–39]. The ligand-grafted NPs were mixed in solution and films were cast, embedding the NPs in the polystyrene matrix. Electron micrographs shown in the SI, demonstrate that the NPs were well dispersed. The mixture was then loaded into a flat stainless-steel sample container (shown schematically in SI) with a circular opening. After the sample was loaded into the cavity, Kapton windows were attached, using Momentive RTV106 high temperature adhesive, to seal the sample. The samples were annealed at 180C in vacuum in 2 different orientations (illustrated in Fig. S2 of the SI) for more than one day (24 hours) before performing the XPCS measurements. In orientation A, the thermal gradient is along the plate-like sample parallel to the long edge of the sample container (henceforth referred to as the z-axis). For the other orientation the thermal gradient was along the x-axis, i.e. normal to the flat face of the sample (orientation B in Fig S2.). XPCS experiments were performed at beamline 8-ID-I of the Advanced Photon Source at Argonne National Laboratory using 7.35 keV

X-rays. Measurements were made for sample temperatures between 120C and 170C, where thermal degradation is not expected to be significant. Some preliminary XPCS experiments carried out on this system of NPs at the LCLS XFEL have been published previously [40].

For most XPCS measurements, the intensity autocorrelation function $g_2(\boldsymbol{q},t)$ is averaged over all directions of $\boldsymbol{q}$ in the y-z plane (see Fig. S2) with the same magnitude q, on the assumption of dynamical isotropy, to improve statistical accuracy of counting. In the present experiment however, the pixels in the 2D detector were grouped into 36 pie-shaped sectors, each subtending an angle of 10° at the center, and whose mean direction to the vertical is given by the angle ϕ. $\phi = 0$ corresponded to the direction parallel to the z-axis, i.e. long edge of the sample container. The g_2 functions were averaged in each sector over pixels corresponding to a magnitude of q within ranges $\pm\Delta q$, where $\Delta q = 9.6\times10^{-4}$ Å^{-1}. Thus, we measured the functions $g_2(q, \phi, t)$.

We begin by discussing measurements made on samples annealed in orientation A. These samples show a progression from normal to anomalous diffusion as the chain length of the PS in the host matrix is increased. For the 18nm Au NPs in the host matrix of MW 13 Kg/mole at 160C the (g_2-1) functions showed no dependence on sector angle at any temperature, i.e. were isotropic, and could be described by a single exponential for $f(q, t)$, with relaxation times $\tau\sim q^{-2}$ as expected for normal Brownian motion, yielding a value of $D = 4450$ Å^2/sec for the diffusion constant at 160C (see Fig. S3 in SI). Then the Einstein-Stokes relation yields for a particle with hydrodynamic radius 9 nm a viscosity of $\sim 8\times10^3$ Poise which is close to the measured viscosity for PS with MW 13 Kg/mole at 160C [41]. This implies normal diffusion in an isotropic viscous fluid, as the host polymer chains can penetrate the ligand brush.

Fig. 1(a) shows the functions (g_2 - 1) measured for the 18 nm Au NPs in the host matrix of MW 30 Kg/mole (close to the entanglement MW) at 160C for $q = 9\times10^{-3}$Å^{-1} for several different angular sectors. One can see that these functions are oscillatory, but that the period of the oscillation is independent of sector angle ϕ so that they are functions only of the magnitude of q.

For the data shown in Fig.1(a), $f(\boldsymbol{q},t)$ can be well described, for all q values, sectors and temperatures in terms of a form for $f(q,t)$ given by:

$$f(q,t) = Ae^{-(t/\tau)^{\beta}}\cos(\omega t) \qquad (5)$$

where β turns out to have a value of ~ 1.8, independent of q and almost temperature independent (see Table T1 in SI). Thus the NP motion is isotropic and $\beta>1$ indicates that it is hyperdiffusive. The prefactor A also turned out to be essentially independent of q, temperature and sample and has a value consistent with the instrumental coherence factor, implying that there is no escape from a cage at very short timescales [23, 26]. For the above system we find that $\tau = (1/v_1)q^{-1}$ and $\omega = v_2 q$, where v_1 and v_2 are constants (see Figs. 1(b) and 1(c)). This corresponds to a ballistic motion of the NPs, with v_2 representing the peak velocity and v_1 the width of the distribution.These turn out to be dependent on temperature and the size of the NP. Similar results were found for the 13 nm diameter NPs.

Next we present results for the host matrix consisting of chains of MW 97 Kg/mole. The dynamics we observed for this case were strikingly different for samples annealed in the horizontal (B) and in the vertical (A) orientations. For the samples containing 18 nm Au NPs annealed in orientation B, the results are very similar to those reported above for the 30 Kg/mole MW host matrix, with isotropic, oscillatory (g_2-1) functions which can be fit with Eq. (5). For these samples $\beta \approx 2$, implying a Gaussian spatial self-correlation function for the diffusing particle with a width that increases linearly with time, as expected for ballistic motion.

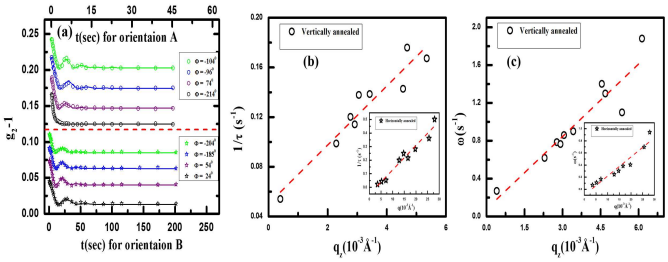

FIG. 2. (a)Relaxation dynamics in terms of g_2 - 1 as a function of τ at different angles ϕ at T=160 C and q=9× 10^{-3} Å^{-1} for sample of 97 Kg/mole host matrix with nanoparticle diameter 18 nm annealed in orientation A (○) and orientation B (⋆), plotted with 2 different time scales as shown. The curves have been vertically displaced for clarity. Dependence of (b) $1/\tau$ and (c) ω as a function of q_z (= $q\cos\phi$) at T=160 C for 18 nm Au NPs annealed in orientation A. Inset panels in fig (b) and (c) represent the cases of samples at orientation B as a function of q.

However, the results for samples annealed in orientation A for the same host matrix of MW 97 Kg/mole are very different. Fig. 2(a) shows the functions (g_2-1) for the 18 nm Au NPs for both annealing orientations for q = 9×10^{-3} Å^{-1} for several different sector angles ϕ. It can be seen that for this orientation these functions are also oscillatory, but in this case the period of the oscillation varies with ϕ. They can be well fitted for all q values, sector angles ϕ and temperatures, with the form for $f(\boldsymbol{q}, t)$ given by Eq. (5), where $\tau=(1/v_1)\ (q\cos\phi)^{-1}$ and $\omega = v_2 q\cos\phi$. Note that $(q\cos\phi)$ is simply q_z the component of $\boldsymbol{q}$ along the z-axis. Thus in this case $f(\boldsymbol{q},t)$ may be rewritten as

$$f(q,t) = Ae^{-(v_1 q_z t)^{\beta}}\cos(v_2 q_z t) \qquad (6)$$

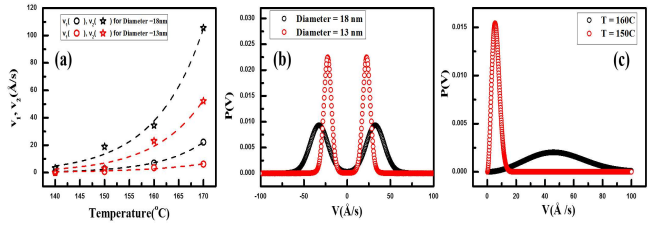

FIG. 3. The variations of (a)v_1 and v_2 for the 13nm and 18nm Au NPs samples with 97 Kg/mole host matrix annealed in orientation A, as a function of temperature. Velocity distributions at T=160 C for NPs in (b) 97Kg/mole and (c) 18nm Au NPs in the 30Kg/mole host matrices annealed in orientation A.

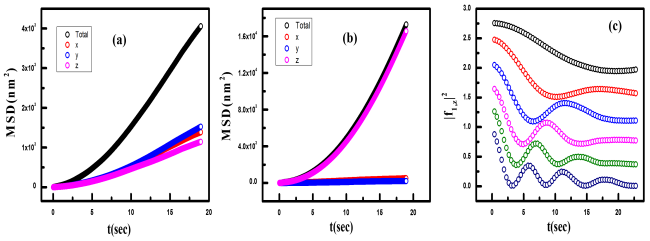

FIG. 4. Mean square displacement (MSD) and ISF computed from simulations (a) Overall MSD as a function of time and its x, y, z components of gold NP in MW = 13 Kg/mol polymer host matrix. (b) Overall MSD and its x, y, z components and (c) ISF modulus square $|f_{1,z}|^2$ as a function of t(sec) of gold NP in MW = 143 Kg/mol polymer host matrix. All f_1 curves are normalized and shifted vertically. Here, q *(n)* = 2πn/(55×45) Å^{-1}.

This corresponds to one-dimensional ballistic motion along the z-axis, with v_1 and v_2 representing 2 characteristic velocities, which are temperature dependent. By Eq. 4, the velocity distributions can be obtained from the Fourier transform of $f(\boldsymbol{q},t)$. Fig. 3 show the isotropic velocity distribution of the 18 nm NPs between v and $(v + dv)$ in the 30 Kg/mole MW host matrix, the velocities v_1 and v_2 for the 13 nm and 18 nm Au NPs as a function of temperature, and the corresponding one dimensional distributions of particle velocities along the z-axis obtained by Fourier transforming $f(q_z,t)$ in the 97 Kg/mole MW host matrix, for samples annealed in orientation A. Paradoxically, the larger NPs have higher drift velocities. We argue that this may be due to the fact that the host matrix chains penetrate even less into the larger NPs which have a higher density of grafted ligand chains, thus providing less resistance to drift motion. In order to confirm this very unusual anisotropic motion of NPs, we repeated these experiments on new but similar samples after a reasonable interval of time, with identical results.

These distributions peak at $v = \pm v_2$. The present results show that the particle motion can be described statistically in terms of a one-dimensional Levy flight [42], with a random distribution of jump lengths, and a drift velocity along the z-axis between jumps, i.e. a Levy walk [43], on a time-scale typically longer than the range of time scales measured for $g_2(\boldsymbol{q},t)$, with a distribution of velocities around $\pm v_2$. This distribution can be described statistically by a Levy stable distribution [32, 42, 43]. As shown in the SI, $P(v\text{-}v_2)$ behaves asymptotically as $(v\text{-}v_2)^{-(1+\beta)}$ as expected for Levy stable distributions. We hypothesize that the one-dimensional motion of the NPs arises from the dynamic alignment of the polymer chains of the host matrix along the z-axis due to the NP motion along the direction of heat flow, during the thermal annealing process in orientation A, as discussed below.

To test this hypothesis, we conducted molecular dynamics simulations of a gold NP diffusing in a polymer melt that is relaxing from a state with pre-aligned polymer chains in the z-direction (see SI for details of calculations) [44–47]. In particular, we examined 2 systems: a single PS-grafted (MW $\sim$ 38 Kg/mol) NP diffusing within an unentangled PS matrix (with short chains of MW $\sim$ 13 Kg/mol) and in an entangled PS matrix (with long chains of MW $\sim$ 143 Kg/mol). During the simulations, the mean squared displacement (MSD) of the NP and its components along the x-, y-, and z- directions were calculated. We also calculated the ISF $f(\boldsymbol{q}, t)$ defined in Eq. (2) for values of $\boldsymbol{q} = (2\pi/L)(n_x,n_y,n_z)$; n_x,n_y,n_z are integers, and L is the size of the simulation box (which was taken to be as large as possible, i.e. 55σ, where σ is the bead size. See SI). This is at least 5 times larger than the hydrodynamic size of the polymer-grafted NP.

We performed calculations of $f(\boldsymbol{q},t)$ with $\boldsymbol{q}$ along the x,y,z directions (which we label $f_{1,x}$, $f_{1,y}$, and $f_{1,z}$ respectively) with n_x, n_y, n_z ranging from 1 to 6. (Values $<$ 1 correspond to wavelengths incompatible with the periodic boundary conditions). In the short-chain PS system, simulations demonstrate a linear trend of the overall MSD with t and almost equivalent values of the MSD in the x, y and z directions (Fig. 4(a)) suggesting normal isotropic diffusive behavior of the NP, as observed experimentally. However, in the higher MW system, the MSD curves are proportional to t^2 over most of the time scale investigated, which corresponds to ballistic motion (Fig. 4(b)), though they eventually become linear at much longer times. The x, y components of the MSD are very small, while the z component is almost identical to the total MSD, implying highly anisotropic motion of the NP along the z-direction. (In the Supplementary Information section, we discuss how the length- and time-scales of the simulations can be mapped onto the length- and time-scales of the experimental measurements).

Interestingly, the simulations also show damped oscillatory behavior of the $f_{1,z}$ curves with time, for different values of q_z (Fig. 4(c), which agree with what is observed experimentally in terms of the number of oscillations ob-

served, the positions and amplitudes of the oscillations, and the overall range of time scales. Our simulation reveals ballistic motion with velocities $v_{sim} \approx 71$ Å/s in the same range as the experiments $v_{exp} \approx 38$ Å/s. The reason that v_{sim} is higher than v_{exp} is likely because the system temperature in the simulations was held fixed at $T \approx 485$ K while it was $T \approx 434$ K in the experiments.

Note that an oscillatory f_1 does not imply oscillatory motion of these particles, but rather confirms the drift like motion. However, following the motion of the particle in the simulations did indicate frequent reversals of the direction of motion of the particle. The corresponding $f_{1,xy}$ curves decay without significant oscillation, indicating that the ballistic motion of the NP is confined to the z direction only. It confirms that this anisotropic motion of the NP can be replicated only in the high molecular weight PS host matrix. Although a rigorous theory is lacking, it is likely that the ballistic motion of the NPs through the higher MW chains of the host matrix (which cannot penetrate the ligand chain brushes on the NPs) is due to thermal gradients and/or release of stresses caused by local distortions in the network. In the case of the 97 Kg/mole host matrix, and samples annealed in orientation A, where the thermal gradient is along the z-axis, this motion can cause dynamical alignment of the host matrix chains. This can be seen by considering the Weissenberg number [48] for this situation given by $Wi = (v_2/D)\tau_m$ where the first factor is the shear rate (v_2 being the NP velocity, D its diameter) and τ_m is the terminal chain relaxation time. Inserting appropriate values for the latter for the 97 Kg/mole PS chain [49], we find $Wi \geq 1$, which can result in chain alignment, as observed, with the particles drifting in both directions along the aligned chains. For the 30 Kg/mole PS chains with faster relaxation times or samples annealed in position B (with no strong thermal gradient), such alignment does not occur, and the resulting motion is isotropic. Movies of the simulation of the motion of the NP within the host polymer matrices may be accessed online (see SI).

In summary, we have discovered cases of novel highly anisotropic ballistic motion with characteristic drift velocities for densely grafted functionalized Au NPs moving in high molecular weight polymer melts. We believe that the cause is dynamical alignment of the chains by the NPs as they move driven by thermal gradients and release of stresses in the network, but to our knowledge, there has been no theory to account for ballistic motion of NPs in polymer networks. The theoretical treatment of Bouchaud and Pitard of jammed colloidal particles moving due to the release of elastic stresses in the medium, characterized by $\beta > 1$ and $\tau \approx q^{-1}$ [50] may be more appropriate to the present case. However, it is remarkable that all these phenomena, are semi-quantitatively reproduced by the molecular dynamics simulations reported here. Together, the experimental measurements and simulations provide a detailed description of anomalous NP motion in an entangled polymer network.

This work was supported by a grant from the Biomolecular Materials Program, Division of Material Science & Engineering, Office of Basic Energy Sciences, US Department of Energy under award number DE-SC0018086. The use of the APS is supported by the U.S. Department of Energy, Office of Basic Energy Sciences, under Contract No. DE-AC02-06CH11357.

* Corresponding author.
† ssinha@physics.ucsd.edu

[1] A. C. Balazs, T. Emrick, and T. P. Russell, Science **314**, 1107 (2006).
[2] R. B. Thompson, V. V. Ginzburg, M. W. Matsen, and A. C. Balazs, Science **292**, 2469 (2001).
[3] S. Srivastava and J. Basu, Phys. Rev. Lett. **98**, 165701 (2007).
[4] Q. Zhang and L. A. Archer, Langmuir **18**, 10435 (2002).
[5] S. Sternstein and A. J. Zhu, Macromolecules **35**, 7262 (2002).
[6] M. E. Mackay, T. T. Dao, A. Tuteja, D. L. Ho, B. Van Horn, H. C. Kim, and C. J. Hawker, Nat. Mater. **2**, 762 (2003).
[7] G. Filippone, G. Romeo, and D. Acierno, Langmuir **26**, 2714 (2009).
[8] H. Wang, C. Zeng, M. Elkovitch, L. J. Lee, and K. W. Koelling, Poly. Eng. & Sci. **41**, 2036 (2001).
[9] S. W. Hsu, A. L. Rodarte, M. Som, G. Arya, and A. R. Tao, Chem. Rev. **118**, 3100 (2018).
[10] M. E. Mackay, A. Tuteja, P. M. Duxbury, C. J. Hawker, B. Van Horn, Z. Guan, G. Chen, and R. Krishnan, Science **311**, 1740 (2006).
[11] L. Cipelletti, S. Manley, R. Ball, and D. Weitz, Phys. Rev. Lett. **84**, 2275 (2000).
[12] R. A. Omari, A. M. Aneese, C. A. Grabowski, and A. Mukhopadhyay, J. Phys. Chem. B **113**, 8449 (2009).
[13] C. A. Grabowski, B. Adhikary, and A. Mukhopadhyay, Appl. Phys. Lett. **94**, 021903 (2009).
[14] S. Srivastava, A. Kandar, J. Basu, M. Mukhopadhyay, L. Lurio, S. Narayanan, and S. K. Sinha, Phys. Rev. E **79**, 021408 (2009).
[15] D. Kim, S. Srivastava, S. Narayanan, and L. A. Archer, Soft Matter **8**, 10813 (2012).
[16] A. C. Genix and J. Oberdisse, Curr. Opi. in Coll. & Int. Sci. **20**, 293 (2015).
[17] H. Guo, G. Bourret, R. B. Lennox, M. Sutton, J. L. Harden, and R. L. Leheny, Phys. Rev. Lett. **109**, 055901 (2012).
[18] T. Koga, C. Li, M. Endoh, J. Koo, M. Rafailovich, S. Narayanan, D. Lee, L. Lurio, and S. K. Sinha, Phys. Rev. Lett. **104**, 066101 (2010).
[19] R. A. Narayanan, P. Thiyagarajan, S. Lewis, A. Bansal, L. Schadler, and L. Lurio, Phys. Rev. Lett. **97**, 075505 (2006).
[20] H. Guo, G. Bourret, M. K. Corbierre, S. Rucareanu, R. B. Lennox, K. Laaziri, L. Piche, M. Sutton, J. L. Harden, and R. L. Leheny, Phys. Rev. Lett. **102**, 075702 (2009).
[21] R. Mangal, S. Srivastava, S. Narayanan, and L. A. Archer, Langmuir **32**, 596 (2016).

[22] S. Narayanan, D. R. Lee, A. Hagman, X. Li, and J. Wang, Phys. Rev. Lett. **98**, 185506 (2007).

[23] A. Grein Iankovski, I. C. Riegel Vidotti, F. F. Simas Tosin, S. Narayanan, R. L. Leheny, and A. R. Sandy, Soft Matter **12**, 9321 (2016).

[24] A. Papagiannopoulos, T. Waigh, A. Fluerasu, C. Fernyhough, and A. Madsen, J. Phy. Condens. Matter. **17**, L279 (2005).

[25] L. H. Cai, S. Panyukov, and M. Rubinstein, Macromolecules **44**, 7853 (2011).

[26] L. H. Cai, S. Panyukov, and M. Rubinstein, Macromolecules **48**, 847 (2015).

[27] B. J. Berne and R. Pecora, *Dynamic light scattering: with applications to chemistry, biology, and physics,* (Dover Publications Inc., 1976).

[28] J. R. Lhermitte, M. C. Rogers, S. Manet, and M. Sutton, Review of Scientific Instruments **88**, 015112 (2017).

[29] F. Livet, F. Bley, F. Ehrburger-Dolle, I. Morfin, E. Geissler, and M. Sutton, Journal of synchrotron radiation **13**, 453 (2006).

[30] S. Busch, T. H. Jensen, Y. Chushkin, and A. Fluerasu, The European Physical Journal E **26**, 55 (2008).

[31] Since $g_2(\boldsymbol{q}, t)$ is $|\mathrm{f}(\mathbf{q}, t)|^2$, a complex oscillatory $f(\boldsymbol{q},t)$ will yield a constant. However, a symmetrical velocity distribution will yield a real $f(\boldsymbol{q},t)$, and thus an oscillatory g_2 function.

[32] L. Cipelletti, L. Ramos, S. Manley, E. Pitard, D. A. Weitz, E. E. Pashkovski, and M. Johansson, Faraday Discussions **123**, 237 (2003).

[33] J. Choi, M. J. Hore, N. Clarke, K. I. Winey, and R. J. Composto, Macromolecules **47**, 2404 (2014).

[34] J. Choi, M. J. Hore, J. S. Meth, N. Clarke, K. I. Winey, and R. J. Composto, ACS Macro Letters **2**, 485 (2013).

[35] A. M. Savage, E. Ullrich, S. M. Chin, Z. Kiernan, C. Kost, and S. R. Turner, J. Poly. Sci. Part A: Poly. Chem. **53**, 219 (2015).

[36] G. Moad, Y. Chong, A. Postma, E. Rizzardo, and S. H. Thang, Polymer **46**, 8458 (2005).

[37] W. Shen, Q. Qiu, Y. Wang, M. Miao, B. Li, T. Zhang, A. Cao, and Z. An, Macromolecular Rapid Comm. **31**, 1444 (2010).

[38] S. Liu, G. Chen, P. N. Prasad, and M. T. Swihart, Chem. Matter. **23**, 4098 (2011).

[39] D. N. Benoit, H. Zhu, M. H. Lilierose, R. A. Verm, N. Ali, A. N. Morrison, J. D. Fortner, C. Avendano, and V. L. Colvin, Anal. Chem. **84**, 9238 (2012).

[40] J. Carnis, W. Cha, J. Wingert, J. Kang, Z. Jiang, S. Song, M. Sikorski, A. Robert, C. Gutt, S.-W. Chen, *et al.*, Scientific reports **4**, 6017 (2014).

[41] J.-C. Majeste, J.-P. Montfort, A. Allal, and G. Marin, Rheologica acta **37**, 486 (1998).

[42] J. P. Bouchaud and A. Georges, Phys. Rep. **195**, 127 (1990).

[43] V. Zaburdaev, S. Denisov, and J. Klafter, Rev. Mod. Phys. **87**, 483 (2015).

[44] K. Kremer and G. S. Grest, J. Chem. Phys. **92**, 5057 (1990).

[45] J. D. Weeks, D. Chandler, and H. C. Andersen, J. Chem. Phys. **54**, 5237 (1971).

[46] E. A. Rakhmanov, E. Saff, and Y. Zhou, Math. Res. Lett **1**, 647 (1994).

[47] E. B. Saff and A. B. Kuijlaars, Math. Intelligencer **19**, 5 (1997).

[48] T. Schweizer, J. van Meerveld, and H. C. Öttinger, Journal of rheology **48**, 1345 (2004).

[49] S. Costanzo, Q. Huang, G. Ianniruberto, G. Marrucci, O. Hassager, and D. Vlassopoulos, Macromolecules **49**, 3925 (2016).

[50] J. P. Bouchaud and E. Pitard, Eur. Phys. J. E **6**, 231 (2001).